AIAA JOURNAL
Vol. 44, No. 12, December 2006

Design of Postbuckled Spinal Structures for Airfoil Camber and Shape Control

Narcis M. Ursache,* Andy J. Keane,† and Neil W. Bressloff‡
University of Southampton, Southampton, SO17 1BJ England, United Kingdom

DOI: 10.2514/1.22636

In this paper the use of shape definition schemes to design spinal structures for the control of deformable airfoils is examined. The aim is to find structures that, when suitably loaded, can be used to alter the aerodynamic properties of a cladding that forms the airfoil, thus obviating the need for flaps or ailerons. Morphing through different cambered airfoils to achieve aerodynamic performances for different maneuvers is then possible by exploiting a range of incremental nonlinear structural solutions. Further, by using structures that are acting in the postbuckling regime, it is possible to obtain significant changes in shape with only modest changes in applied load. Results are formulated in terms of the aerodynamic properties of the morphed airfoils using a shape optimized beam as the spinal structure with fixed aerodynamic cladding.

I. Introduction

THE availability of new technology and improved analytical tools has opened up many new possibilities for multistructural systems. Smart aerostructures and compliant control surfaces have consequently become a potential way forward in the development of adaptive wings. Modern wing morphing concepts require a structure within the wing that can continuously change the shape of the wing in flight to alter the flow stream and achieve enhanced or changed aerodynamic properties, without the hinge contour discontinuity associated with articulated surfaces. There is a great deal of current interest among aircraft designers in such shape control systems, primarily because engineers seek designs that have low radar or acoustic signatures. By removing hinged control surfaces roll performance and reversal speed can also be improved [1,2].

Flapless, variable geometry airfoils are not a new idea. The original Wright Brothers Flyer used a "wing warping" concept to provide control, following developments with gliders [3]. Ailerons had not been invented at that stage and the brothers suggested that their approach would provide benefit in flying an aircraft. Their control system worked by pulling on a set of external steel wires which twisted the wing tips relative to the rest of the wing.

Since the early 1980s, researchers have investigated the use of fully integrated *smart structures* for performance and shape control of deformable flight devices. In these, the wings become adaptive in the sense that they can change profile to adapt to flow conditions by controlled transitions from one airfoil shape to another. Deformable surfaces can also be replaced by microsurface effectors (e.g., piezoelectric actuators) or fluidic devices (i.e., synthetic jet actuators), offering further potential for controlling the baseline aerodynamic characteristics of the airfoil.

Schemes have been proposed to enhance flow conditions over wings by adapting the aerodynamic shapes through translation actuators placed in the rib stations spanwise [2,4]. Such approaches for morphing wing sections require an optimized distribution of forces and reliable and lightweight actuators. The investigation of synthetic jet actuators has been considered for manipulating flight control characteristics and flow separation [5,6] by interacting the streamlines with a jet generated by miniature surface-mounted devices, inducing an apparent change in shape. Highly compact actuators using smart materials have also provided a means of changing shapes and controlling structures, and mitigated some of the weight penalties of other approaches. Various schemes that induce strain in structures have been built using smart memory alloys (SMAs) and piezoelectric actuators, and used to adjust the thickness of airfoils to control flow separation [7,8], also to offer high precision operation and finite deformation in antenna reflectors [9,10]. These approaches offer reliable alternatives to complex and heavy wing structure controllers, but they have limitations in terms of power and deformation. The use of smart structures such as compliant mechanisms also provides a viable approach to achieve local shape deformation of systems and a more limited number of actuators is then needed to control the strain energy transmitted to the deformable shape [11,12]. For example, locally buckled skin structures have been considered for shape control of specific regions of airfoils by Natarajan et al [13].

A number of these ideas have been tested in practical applications, for example the Mission Adaptive Wing [14] and the Active Aeroelastic Wing (AAW) [15]. The AAW was used on an early version of the F-18 fighter to provide enhanced flight characteristics at supersonic speeds by controlling the induced strain in structures with piezoelectric actuators. The morphing concept also has significant applicability for Unmanned Air Vehicles (UAVs), to enhance their maneuverability and cope with complex-role missions with an inherent tradeoff with regard to endurance and range (e.g., buckle-wing [16], torque-rod actuated wing [17]).

The primary focus of the research presented here is to develop new means of achieving deformable airfoils, by using the concept of spinal structures first introduced in [18]. The methodology proposed in this paper involves both structural and aerodynamic optimization with respect to the geometry of the airfoils under different flow conditions. The aerodynamic features are defined by a cladding of hyperelastic material, which is continuously deformed by the central spinal structure. Key assumptions are that the volumetric response of this material is low, so as to avoid flaws in the outer surface of the airfoils during morphing, and also that the structural strength of the airfoil, provided by the deforming spinal structure, is sufficient to prevent aerodynamically induced deflections. The structural stability of the setup, including the postcritical regime (i.e., postbuckling) is included in the design process to allow for large displacements (i.e., of the order of a camber of the airfoil) with modest changes in strain energy.

Received 25 January 2006; revision received 7 April 2006; accepted for publication 1 July 2006.

*Research Student, Computational and Engineering Design Group; narcisu@soton.ac.uk.

†Professor, Computational and Engineering Design Group; ajk@soton.ac.uk.

‡Senior Research Fellow, Computational and Engineering Design Group; nwb@soton.ac.uk.

II. Shape Control Concept

Wing morphing technology involves changing control surface shapes during flight to provide varying aerodynamic properties (i.e., for changes in mission or maneuver). The means of airfoil reshaping presented in the literature mainly focus on targeted local changes using a flexing outer skin (see, for instance, [11,13]). A flexible outer skin is also adopted here, but in contrast to much of the work reported in the literature, the entire airfoil ship is altered. This global reshaping is achieved by distorting a slender internal spinal structure which is attached to a hyperelastic outer cladding that forms the aerodynamic surface of the morphed airfoil. Because each maneuver during flight may require a different camber configuration, the system proposed here morphs through a significant camber range using an incremental loading scheme. This allows a series of target aerodynamic shapes to be realized (in this study a set of NACA-four digit airfoils), see later in Fig. 3.

The spinal structure considered is a simply supported Euler strut subject to an eccentric load, as depicted in Fig. 1 (n.b., the eccentricity is exaggerated in the figure to highlight the asymmetrical nature of the loading). The unloaded strut is connected to a flexible outer cladding of airfoil shape via a foam core (here a baseline uncambered NACA-four digit thickness definition is chosen for its analytical simplicity). This provides a datum symmetrical shape, with the camber line identical to the neutral fiber of the spinal structure. To change this shape the strut is loaded and allowed to buckle so that the camber line of the airfoil is then curved, taking the foam core and entire outer skin with it. Obviously, if the strut were uniform this would lead to a half sine wave spinal shape (given by the first structural eigenmode [18]) whose amplitude is intrinsically controlled by the end point load: such a curve is not very helpful as a camber line although, given the airfoil shaped foam core proposed, a range of airfoil shapes with varying cambers is nonetheless generated. If, however, a strut with varying structural properties is used (for example, varying lateral stiffness, material, etc.) the strut ceases to take up such a simple deflected shape when loaded. By suitable choice of material properties more realistic camber profiles can then be generated. This naturally leads to an inverse structural design problem that can be solved to achieve NACA-like (or any other) camber shapes and thus a range of suitably cambered airfoils. Because for airfoil definitions like the NACA series, the overall aerodynamic shape is separable between thickness distribution and camber line, this means that the morphing process can be made to sweep through an entire NACA series provided the spinal structure deflects through the required series of camber shapes. Moreover this series of shapes is generated using a single actuator: control simplicity being achieved by structural sophistication. It is noted in passing that this basic idea could also be applied to control of twist or dihedral by using appropriately placed struts.

Fig. 1 Structural setup for morphing shape optimization.

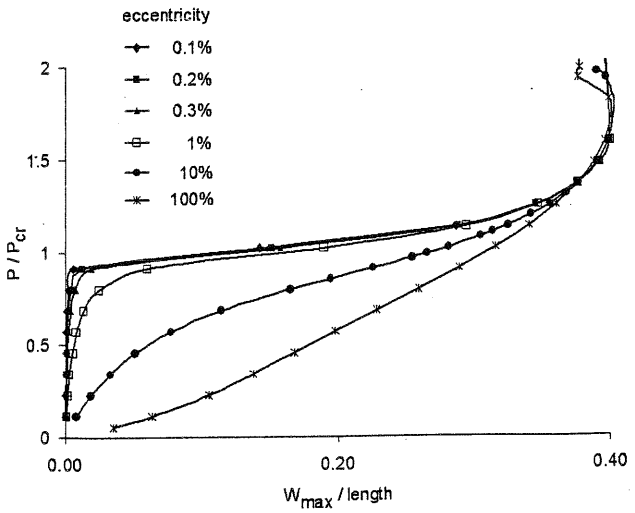

Fig. 2 Sensitivity of regular struts to eccentricity of loading.

As well as overall shape control, the adoption of a buckled spinal structure allows for changes in shape with modest force levels. Figure 2 shows the impact of end forces for struts with varying degrees of eccentricity in their end loading. It is clear that if the end loads are varied at levels close to the critical Euler buckling load then large deflections can be achieved with modest changes in end force level. Therefore, in the work presented here the structural systems proposed are all operated with forces close to their critical loads. Because the aim during operation is to move the spinal structure smoothly between a series of predefined camber line shapes it is necessary to find structures that deform through such shapes during their postbuckling behavior: this is, of course, more difficult than finding a strut that produces a single desired camber line at one fixed load value. To solve this problem a nonlinear finite element analysis (FEA) is performed using an incremental loading scheme [19–21], with a static equilibrium being obtained after each load increment. This allows the full range of shapes possible for any particular material layout to be assessed. Then, during design, optimizers are used to try and match these shapes to a series of NACA camber-lines by adjusting the properties of the strut. [It has been found that an additional structural restraint (i.e., rotational spring) is needed for cambers larger than 12% chord. This controls the gradient of the lateral deformation towards the pinned end of the strut, and, by augmenting the stiffness of the structure, has a significant effect on the pre- and postbuckle pattern response.] Inevitably such matches cannot be perfect throughout the range of loading but surprisingly good agreement can be achieved so that the resulting sequences of wing morphs are remarkable close to the desired airfoil shapes. The quality of these shape sequences are here assessed using full potential computational fluid dynamics (CFD) simulations and compared with those of the target airfoils. Even when there are slight differences between the shapes considered, the differences in the resulting pressure distributions are modest. To minimize such differences, a second optimization process can be entered which seeks to further refine the structural design by minimizing differences between desired and achieved pressure distributions, requiring linked CFD and structural analyses.

It should be noted that throughout this work it is assumed that the foam core exhibits a minimal volumetric response and that the aerodynamic loadings on the flexible skin can be ignored compared to the forces and restraint provided by the spinal structure. Clearly any practical structural morphing system would need to be engineered so that aerodynamic loads did not significantly distort the morphed geometries. It is shown later that, for the struts used here, the aerodynamic forces cause acceptably small deformations.

III. Design Strategies

Optimization tools provide a means to achieve better devices during a shape design process, involving strategies such as *direct analysis* or an *inverse approach*. In the first case, one studies the effects of parameter variations via an objective function which is formulated with respect to some target performance metric (such as low drag). Typically the parameterization of the design space is in the form of geometric quantities. Constraints can be structural in nature (e.g., mechanical stability, manufacturing requirements) or aerodynamically related (e.g., desired lift coefficient, etc.). This method is easy to implement due to its simplicity, but often requires a significant number of iterations (i.e., analyses) with no guarantee that the optimized shapes achieve desired performance levels. The inverse approach works towards a given shape by attempting to push some derived characteristic towards a desired configuration. The derived characteristic is usually specified as a field variable (e.g., static pressure or freestream flow) that is, a priori, known to yield desirable performance. Inverse methods are useful when designing

systems with specific characteristics, as undesirable physical effects such as shocks or flaws in shapes can be explicitly avoided. The main difficulty lies in choosing the target performance of the parameterized model.

A large number of papers dealing with optimal design problems via inverse strategies can be found in the literature. A typical goal in inverse structural design is achieving meaningful shapes that conform to specified boundary conditions and fulfill functions such as structural integrity with acceptable performance (e.g., acceptable nominal stress). A significant body of work on the stability of structures subject to displacement and stress constraints has been developed since the early 1970s, as noted in a survey by Haftka and Prasad [22]. This has been followed more recently by studies on optimality criteria with displacement and stress constraints using more powerful numerical algorithms [23], from maximizing the minimum critical load or natural frequencies [24] to stability of imperfection-sensitive structures in the postcritical regime [25]. The optimization of geometrically nonlinear structures is limited with respect to shape and boundary conditions and requires a good understanding of the target structural shape. A general methodology for inverse design for simple structures has been proposed by Bernitsas and Suryatama [26]. Their goal was to achieve improved structures (e.g., reduced vibration amplitudes), subject to various dynamic excitations. The algorithm was formulated as a two-stage problem: a perturbation approach, where the topology/shape points are defined (e.g., static deflections, stress constraints, etc.) and a numerical algorithm to optimize the initial structure following the designer's specifications; this approach has applicability to fluid-structure interactions [27].

The earliest approaches to aerodynamic shape design appear to be by inverse design, back in the midforties, based on *conformal mapping* [28–32], followed by *stream-function-coordinate modeling* [33,34], which are relatively fast, but limited to specific flow models and requiring dedicated coding. The *surface approach*, which links changes in pressure to curvature using semianalytic formulae, has been successfully applied to two-dimensional Euler and Navier–Stokes algorithms, but is less successful when dealing with three-dimensional problems with crossflow characteristics because the curvatures and slopes are computed plane by plane [35,36]. The inverse design method proposed here is similar to this work, in the sense that a target field variable (here the deformed structural shape), is achieved by an iterative upgrade of the design via the design parameters. In this case, however, the target shapes are specified initially by means of existing airfoil camber lines with known properties. Only when good candidate designs have been achieved is attention switched to optimization using aerodynamic properties. This two-stage approach considerably speeds up the design process.

IV. Optimization

As already noted, the primary goal here is the control of aerodynamic shapes by solving a series of structural optimization problems. These problems are tackled using a genetic algorithm (GA) taken from the Options design exploration toolkit[§] to manipulate the structural designs, seeking to match deformed shapes to specific camber lines, i.e., no aerodynamic calculations are used at this stage. GA methods have the advantage of not requiring gradient information and this is important when large variations in geometry are being considered during the initial calculations of the optimization process. They are, however, not at their best when converging to final designs, when gradient-based schemes are to be preferred [37]. In the process used here the best design after 100 generations of the GA, each of 50 members, is taken to be the initial optimum and analyzed using CFD. Subsequent fine tuning of such designs is carried out using gradient-based schemes applied to aerodynamic results coming from CFD. This process involves much smaller design alterations and so is well suited to gradient-based approaches: here a dynamic hill-climbing scheme is taken from the Options toolkit.

During the first stage of design the geometrically nonlinear behavior of the structure is optimized with respect to its deformed shape, allowing for instabilities in the nonlinear response, such as snap-through or snap-down, which can arise from widely varying flexural stiffnesses and end rotational restraints. These instabilities are checked against the load proportionality factor which can exhibit one or more limits and/or turning points before achieving the final cambers of interest. This process requires some care when setting up but can be directly handled using commercial FEA codes (here Abaqus®). The global load control algorithm used to solve the nonlinear problem posed breaks the simulation into a number of increments, for each of which a stable equilibrium is achieved by minimization of the residual force. This allows the optimization problem to be stated in terms of the deflected shapes of the strut after each load increment as

Minimize

$$f(x) = \frac{1}{n_{\text{inc}}} \sum_{i}^{n_{\text{inc}}} \sqrt{\sum_{j}^{n_p} \left[w_{i,j}^{\text{target}}(x) - w_{i,j}^{\text{opt}}(x) \right]^2} \tag{1}$$

Subject to

$$^1 g_i(x) = \max |_j w_{i,j}^{\text{opt}} - a_2 \leq 0 \tag{2}$$

$$^2 g_i(x) = a_1 - \max |_j w_{i,j}^{\text{opt}} \leq 0$$
$$x \in X, \quad \forall\, j \in \{1, \ldots, n_p\}, \quad \forall\, i \in \{1, \ldots, n_{\text{inc}}\} \tag{3}$$

where $X = \{x \in \Re^n | x_k^{\min} \leq x_k \leq x_k^{\max}, k = 1, \ldots, n_v\}$ with $x_k^{\min}$ and $x_k^{\max}$ being bounds on the n_v structural variables set by the user. $w_{i,j}$ are the deflections at load increment i and structural location j, and $a \in \{a_1, a_2\}$ define lower and upper displacement constraints at each load increment, with a maximum number of increments n_{inc}, for each airfoil defined at n_p structural grid points. Note that $w_{i,j}^{\text{target}}$ are chosen from the target camber lines by selecting cambers that have similar overall maximum deflections to those arising at any specific load increment: this further speeds up the design process because it is then no longer necessary to know the specific control force needed to achieve a given shape. For the structures considered here which are of 1 m length and 8 mm width, typical end forces are in the range 40–90 N, with variations of less than 2 N being needed to deflect the camber from 5 to 10%, typically around 2% changes in end force being needed. Of course, for any practical design account would need to be taken of any structural deflections that might be caused by aerodynamic forces. As will be shown later, here such loadings have only a slight effect on the strut deflections. Note also, that although this study is restricted to rather moderate changes in camber, the concept can be shown to work for cambers of up to 25%, which being applied to the whole wing surface would provide all the control authority needed for quite dramatic maneuvers. Designing for such large camber changes does, however, lead to the need for considerably more sophisticated CFD than presented here, and so is left for a future publication.

V. Parameterizations

To optimize the design of the spinal structure, some form of parameterization scheme is needed to link the optimizer to the structural properties of the spine. Robust geometry parameterizations techniques have been available in literature since the late 1970s; see, for example, the survey provided by Samareh [38]. Here two of the better known methods are adopted.

A. Discrete Approach Technique

First a discrete approach (DA) was adopted, using a subset of the finite element grid point coordinates in the structural model to define

[§]See http://www.soton.ac.uk/~ajk/options/welcome.html [cited 1 April 2006].

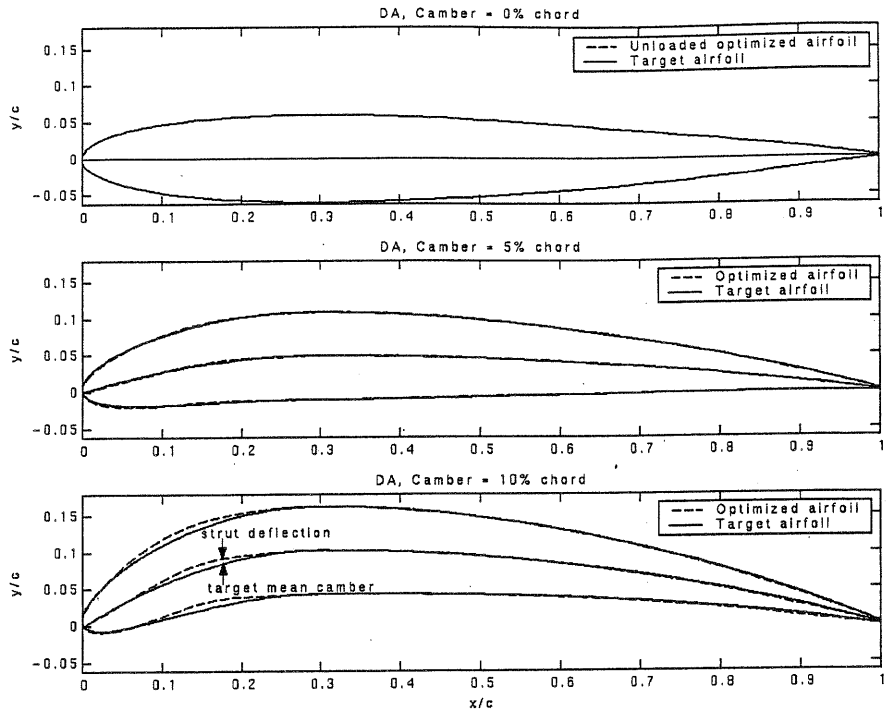

Fig. 3 Baseline plus target and computed airfoils for morphing-optimized beam (DA).

the regions for application of design variables. To allow for a wide range of possible shapes the cross-sectional areas of 12 sections of the spinal beam were varied by parameterizing the thickness distribution along its length (as depicted in Fig. 4: note that the width of the spine is held fixed at 8 mm). The resulting design is used as to achieve aerodynamic shapes by applying a fixed, NACA-based 12% thickness distribution to yield the morphed shape. Although the optimization problem may be readily set up in this way, the resulting structural geometry lacks smoothness and is somewhat impractical to manufacture. Typical cambered shapes resulting from this scheme (i. e, at 5% and 10% camber) are shown in Fig. 3, along with the target NACA sections used in the inverse design and the baseline, undeflected shape.

Instabilities may occur in this approach during optimization due to the widely varying stiffnesses of adjacent elements. Sometimes the global stiffness becomes singular at limit points, diminishing the accuracy of the solution in that region, in which case the structure collapses or "snaps" to another equilibrium phase (i.e., snap-through, snap-down). Therefore postcritical response checking for such instabilities is included as a constraint function by applying feasibility bounds for maximum lateral deflection for each load increment (i.e., $a_1 = 2\%$ and $a_2 = 15\%$ of initial beam length). It is noted that difficulties in detecting and traversing bifurcation and limit points have been a challenge for postbuckling and postcollapse analyses since early 1970s and have led to the development of the arc-length control and alternating load-displacement control methods for handling cases where the response is unstable during part of its loading history [19–21].

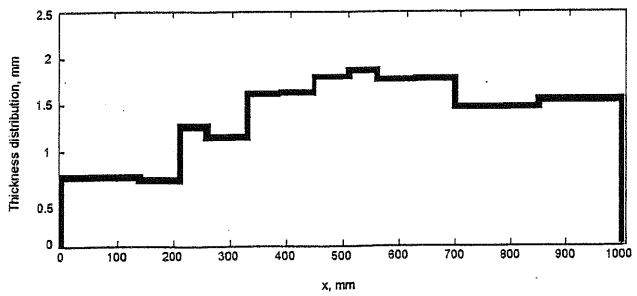

Fig. 4 Morphing-optimized beam (DA): semithickness.

B. Nonuniform Rational B-Splines Approach

CAD systems are now a reliable and accepted engine for MDO processes. Using such tools, complex curved geometry designs based on basis functions can be modeled using the control parameters of nonuniform rational B-spline (NURBS) curves as design variables (see, for example, [39]). This provides great flexibility over the design process at a relatively low cost. Here control of the beam was achieved by manipulating an interpolating NURBS-based parameterized curve using Catia® V5R13 and then transferring this geometry to the FEA analysis as a thickness distribution. This involved moving six evenly spaced points in both x- and y-directions (see [40] for a more detailed discussion of the algorithms behind CAD packages). The optimized shapes produced are very similar to the DA-based designs (see Figs. 3 and 5), but have reduced variations in consecutive flexural stiffness, allowing for slightly smoother aerodynamic designs; see Fig. 6. Note, however, that even a stepwise irregular beam deflects into a shape with at least curvature continuity: this is a key feature of using the structural system in this way. The similarity in shapes between Figs. 4 and 6, produced by these very different parameterizations, suggests that the structural solution to the camber matching problem is not highly multimodal and that either form presents a good basis from which to make further refinements: this is perhaps to be expected because the first buckled mode of a strut is always a well-defined shape, i.e., the problem is well posed structurally, even if occasionally tedious to solve.

Because of the limitations of space, and because the airfoils generated by the two parameterization schemes exhibit such a close agreement in terms of their aerodynamic behavior, only the DA-based airfoil is discussed further here.

VI. Aerodynamic Performance of Morphing Sections

As the shape of an airfoil changes, the flow around it also changes. This leads to an altered pressure distribution, which, in turn, modifies the aerodynamic properties of the model. Here a two-dimensional viscous coupled finite difference code that solves the full potential equations, VGK [41], is used to predict the aerodynamic properties of the morphing airfoils. A standard setup in terms of Mach number and angle of incidence has been built for the target and parameterized airfoils. This covers Mach numbers between 0.4 and 0.8, freestream incidence between -5 and $+10$ deg, and is for a fixed Reynolds number of 5×10^6, transition location 0.03 and shapes with between

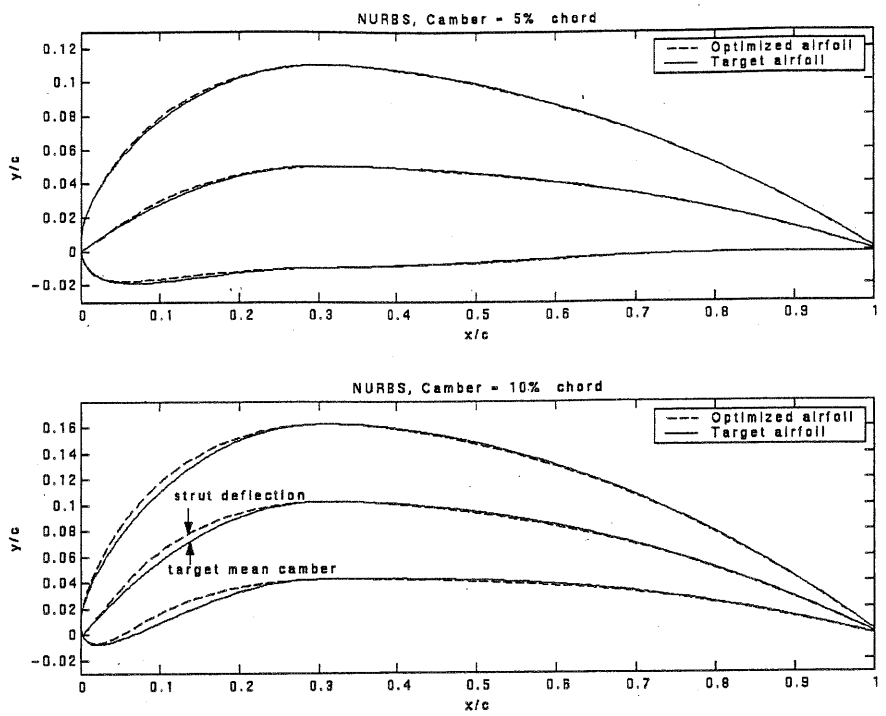

Fig. 5 Target and computed airfoils for morphing-optimized beam (NURBS).

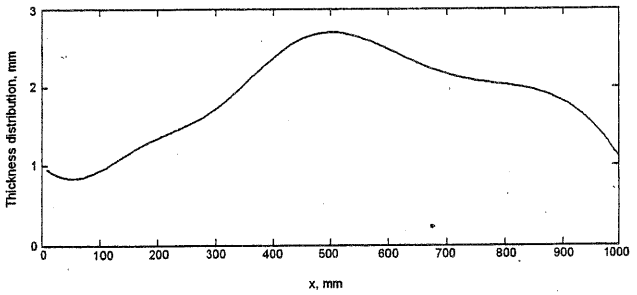

Fig. 6 Morphing-optimized beam (NURBS): semithickness.

2% and 15% camber to chord ratio. VGK provides good accuracy for flows with weak shocks and attached boundary layers and fair predictions of local and overall parameters when the upstream Mach number just before weak shocks does not exceed 1.3.

Flows with these parameters have been studied for the airfoils considered over a range of incidences at Mach 0.4 in order to assess the agreement between the target and optimized airfoil pressure distributions (see Fig. 7). Here a slightly lower pressure on the upper surface of the optimized airfoil is achieved for higher incidence, which leads to slightly enhanced lift. Good agreement in terms of pressure distribution, including the shock position is achieved for mild flight conditions (i.e., $M = 0.4$ and α ranging between -4 and

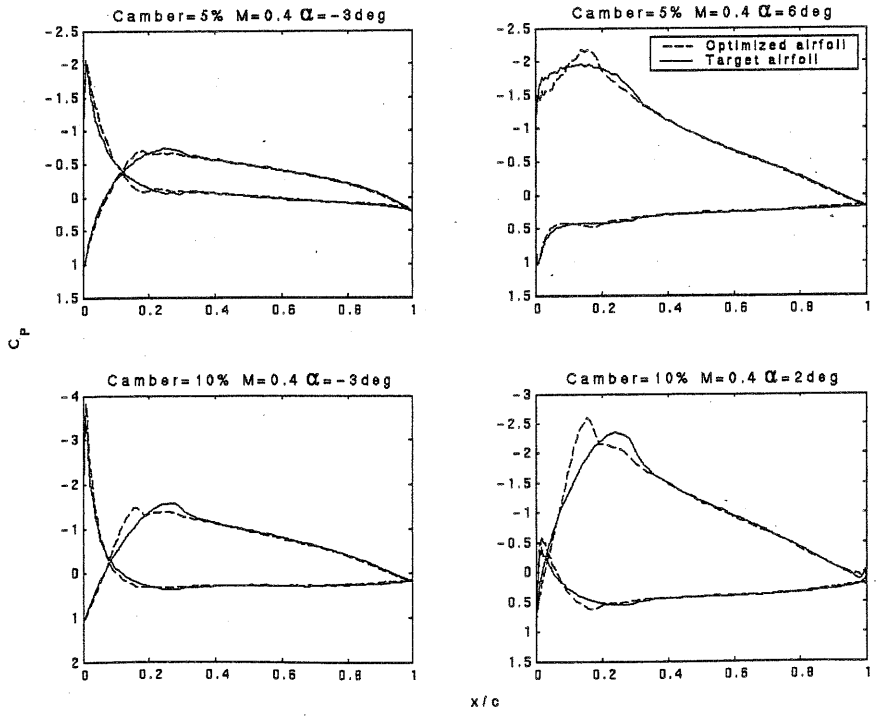

Fig. 7 Pressure distributions for morphed and target cambered airfoils, under mild flow conditions.

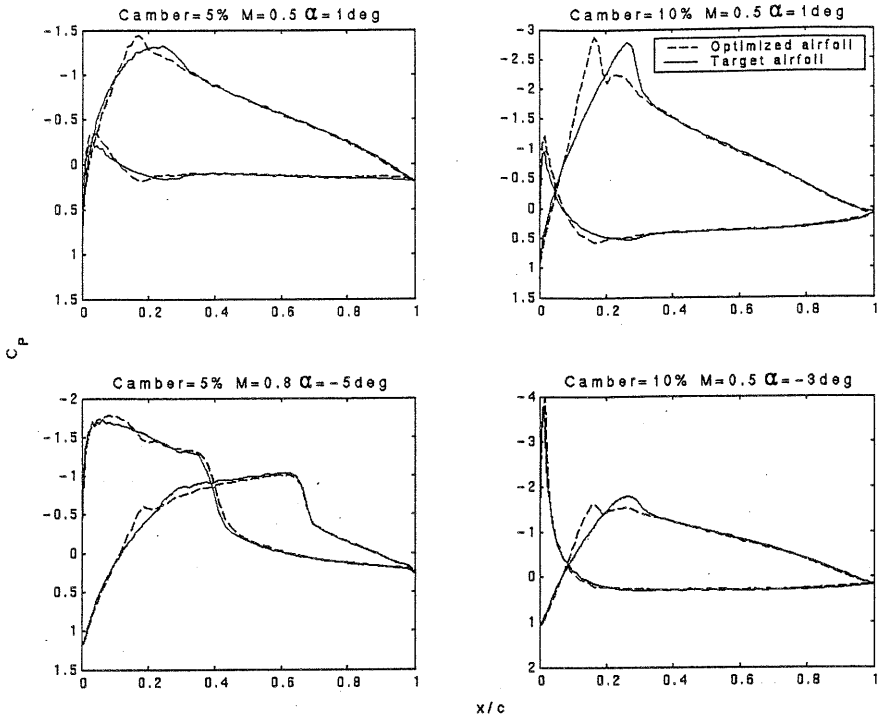

Fig. 8 Pressure distributions for morphed and target cambered airfoils, under mild and more severe flows.

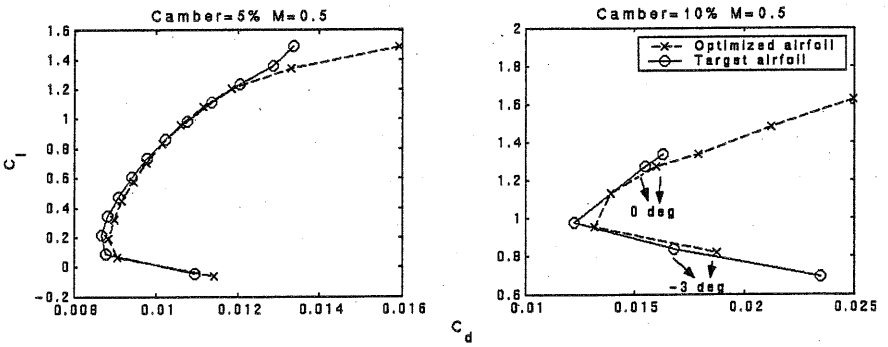

Fig. 9 Drag polars for different cambers.

+6 deg). Note also the slight lack of smoothness in the target pressures for α of +6 deg is damped out by the inverse process by the geometry definition process being used.

Figure 8 shows similar results for slightly more extreme operating conditions, including one at $M = 0.8$, whereas Fig. 9 shows drag polars at $M = 0.5$. Clearly, the pressure distributions are sensitive to changes in geometry, flow parameters, and boundary-layer growth and the flow can readily degenerate into a weak shock for higher cambers and transonic conditions, contributing wave drag. The 5% cambered airfoils, under mild flow regimes show good agreement in terms of pressure, whereas the 10% airfoil results are slightly less good, with a weak shock on the upper surface. As the camber increases, the tendency to upper surface boundary-layer separation becomes more significant, as shown in Fig. 8 for 10% camber at $M = 0.5$ and $\alpha = 0.2$, with shocks at $x/c_{\text{shock},o,u} = 0.1992$, $x/c_{\text{shock},o,l} = 0.0221$ for the optimized airfoil and $x/c_{\text{shock},t,u} = 0.313$, $x/c_{\text{shock},t,l} = 0.0232$ for the target. Even so, relatively good agreement between the two airfoils is achieved in terms of pressure distribution (see Figs. 7 and 8). The drag trends are similar across a wide range of incidences, with particularly good agreement for the low camber point. When morphing between the two camber shapes analyzed in these plots, good aerodynamic performance is obtained throughout. Moreover, the differences in the drag polars seen at 10%

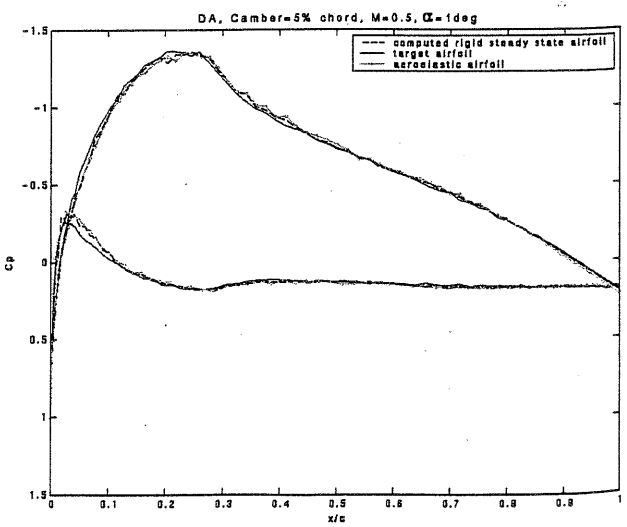

Fig. 10 Pressure distributions for aerodynamically loaded, morphed, and target cambered airfoils.

camber in Fig. 9 can be considerably reduced by a further stage of design optimization which is considered later.

A. Deflections Due to Aerodynamic Loading

To illustrate the impact on these design of the aerodynamic loading a brief study has been conducted on a 5% cambered airfoil at $M = 0.5$ and α of 1 deg. During this study the lift forces acting on the section were applied to the finite element model of the spinal structure and the CFD code used to reassess the camber shape with resulting additional deflections, using a recursive approach with underrelaxation (see Cai and Liu [42], Alonso et al [43]). Figure 10 shows the pressure plots for the aerodynamically loaded design, the unloaded morphed design and the target for this case: as can be seen the effect of the aerodynamic loading is essentially negligible.

B. Design Refinement Using CFD-based Inverse Optimization

To achieve a better aerodynamic agreement than that shown in Figs. 8 and 9, a further optimization procedure can be used to refine the designs. To do this a new optimization criterion is specified in terms of the pressure distribution as follows:

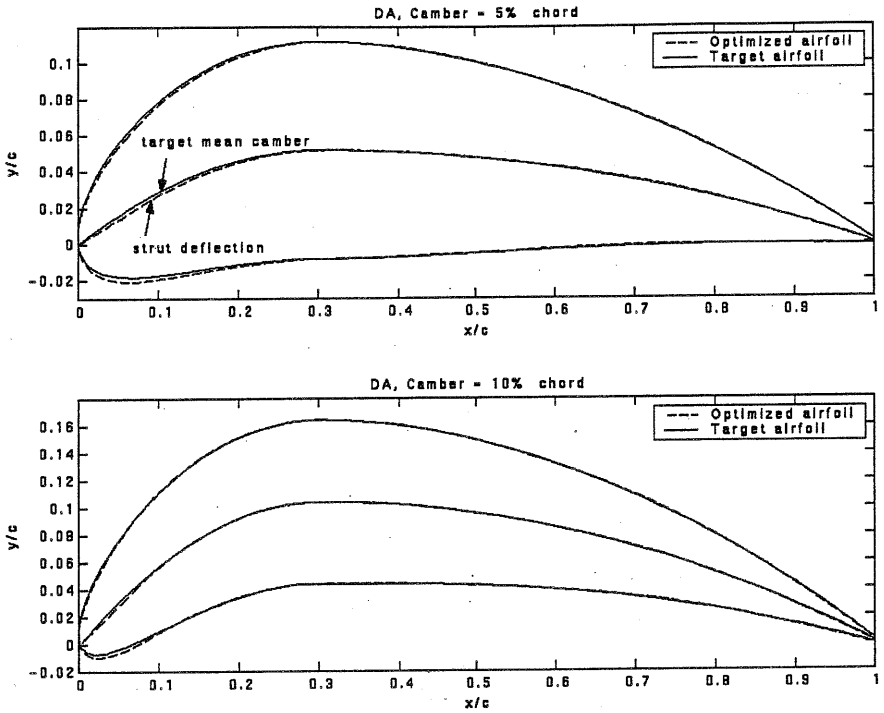

Fig. 11 Target and computed airfoils for morphing-optimized beam after CFD-based optimization.

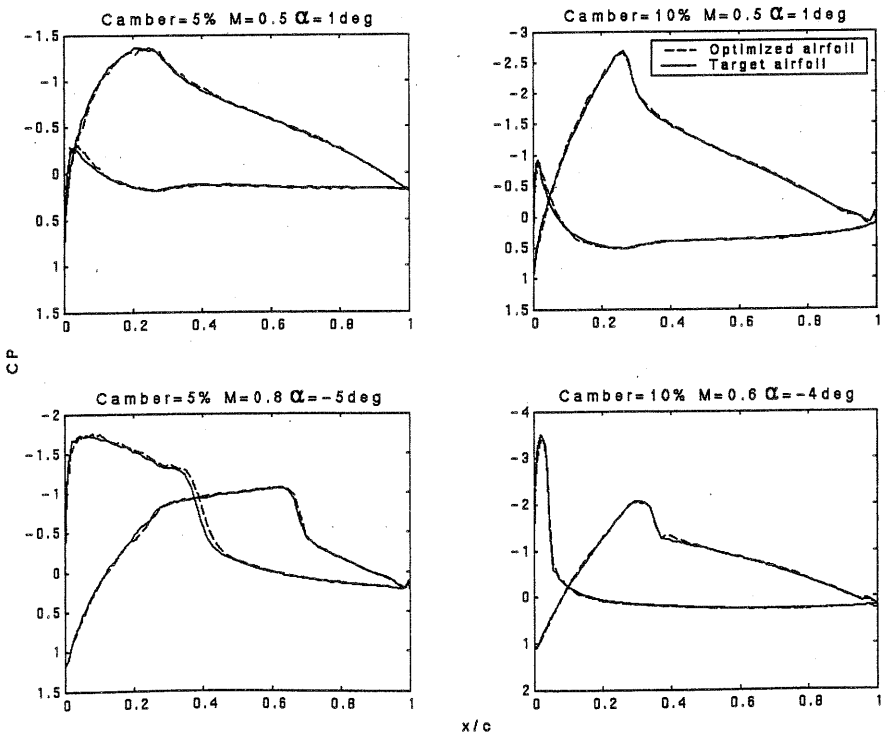

Fig. 12 Refined distributions for morphed airfoils, under mild and extreme flows.

Minimize

$$f(x) = \frac{1}{n_p}\sqrt{\sum_{j}^{n_p}\left[c_{p_j}^{\text{target}}(x) - c_{p_j}^{\text{opt}}(x)\right]^2} \qquad (4)$$

$$x \in X, \quad \forall\, j \in \{1, \ldots, n_p\}$$

where $X = \{x \in \Re^n | x_k^{\min} \le x_k \le x_k^{\max}, k = 1, \ldots, n_v\}$ with $x_k^{\min}$ and $x_k^{\max}$ are bounds of the n_v structural variables set by the user, c_{p_j} is the pressure coefficient distribution computed at location j related to an airfoil defined at n_p points. It would, of course, be possible to use differences in the computed lift and drag rather than in the pressure distribution but this would not enforce agreement between the actual and target shapes over the entire section under study.

As already noted this refining optimization process is driven by a dynamic hill-climbing, gradient-based method to carry out a local search, using as a starting solution the best design from the previous optimization. Here 1600 design evaluations are used and this further improves the geometric matching, see Fig. 11. A very good agreement in terms of pressure distribution, including the shock positions for the higher camber then results (see Fig. 12). This also yields more closely matching drag performance (Fig. 13). The improvement in the matching of the drag polars seen in this figure, compared to that in Fig. 9, justifies the significant extra effort required for the CFD-based optimization, and serves to ensure that good drag performance is maintained while still allowing significant camber control. This is a particularly important feature of the design process, because any gains achieved from flapless control in terms of stealth or reduced noise must not be achieved at the expense of deteriorating aerodynamic behavior. Of course, it would be possible to carry out the entire optimization process using the combined structural and CFD analysis throughout, but this would be considerably more costly than the two-stage process used here. Current work is examining the use of a number of more refined response surface based optimization schemes to further speed up the design process [44].

C. Effect of Foam Core Deformations

Finally, attention is briefly turned to the cladding material assumed in this work. Thus far the core and skin have been modeled by assuming that they can be represented by a fixed thickness distribution taken from the NACA definitions. Here we briefly analyze the behavior of a more realistic model based on a two-dimensional

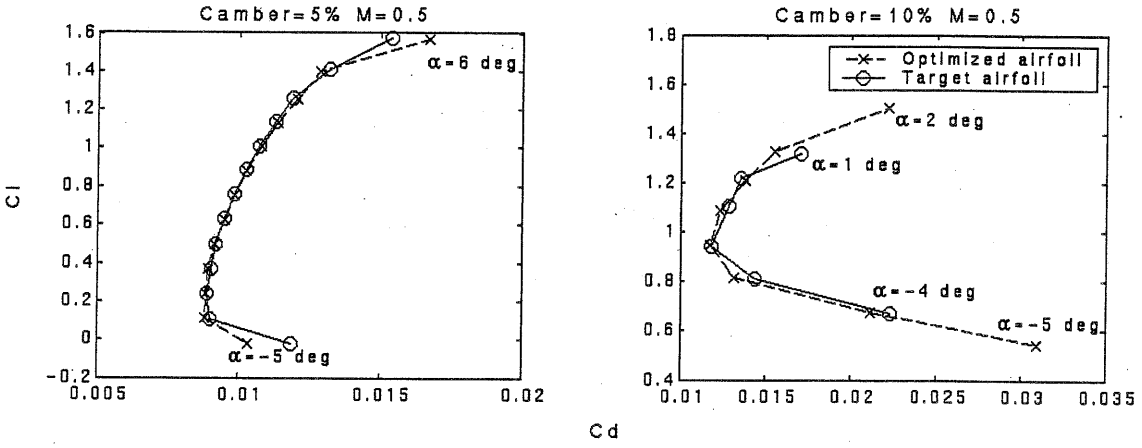

Fig. 13 Refined drag polars for morphed airfoils.

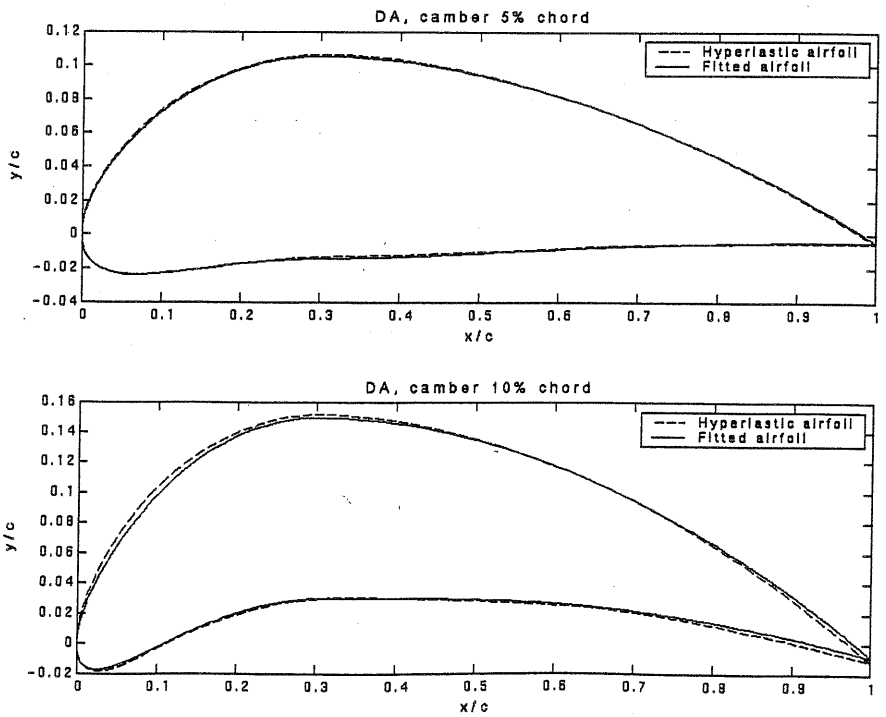

Fig. 14 Foam core model for morphed airfoils under aerodynamic loading.

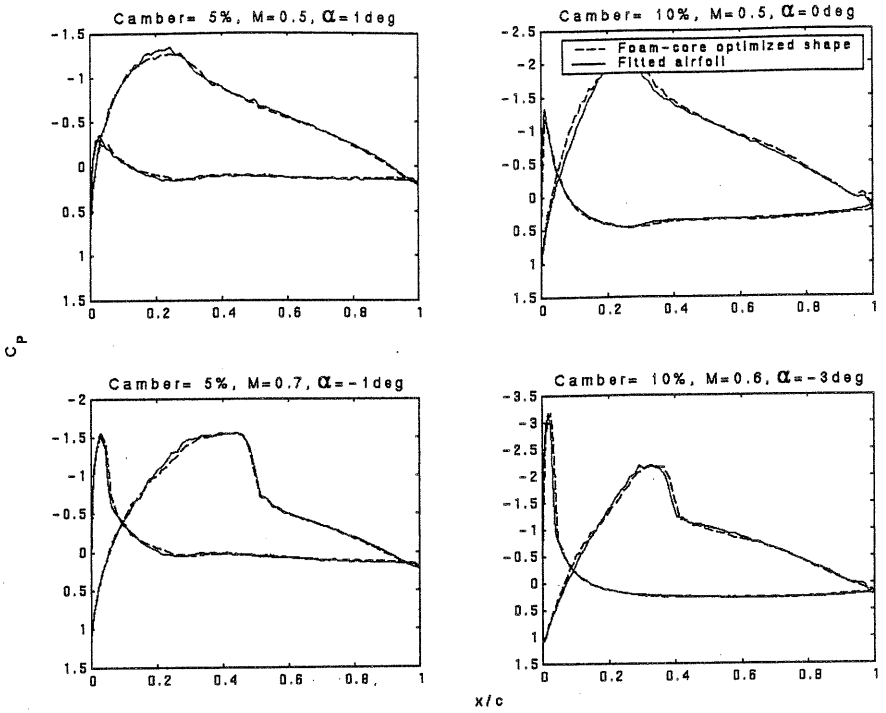

Fig. 15 Pressure plots for foam core model of morphed airfoils.

finite element simulation of a representative elastomeric foam, subject to the aerodynamic pressure loadings used in the design process, attached to the buckled strut model. Clearly, this model is computationally much more expensive than that used during the previous optimization processes, but it does demonstrate the complete configuration allowing for spine and cladding with both control and aerodynamic forces present. Figure 14 shows the resulting shapes from such a study on the CFD optimized foils already shown in Fig. 11. As can be seen the impact on the shapes is relatively minor and study of the resulting pressure plots allowing for this change confirms that the assumption of fixed thickness distribution made during the search processes can be supported, see Fig. 15. Clearly, it would be interesting to carry out a full aeroelastic and flutter analysis for this configuration and this is the subject of ongoing work.

VII. Conclusion

The focus of this research has been to find a means to alter the global aerodynamic performance of an airfoil by controlling its deformable shape. The aim was to find structures that, when suitably loaded, can be used to alter the flow on a cladding that forms the airfoil. Further, by using structures that are acting in the postbuckling regime, it is possible to obtain significant changes in shape with very modest changes in applied load. A very good agreement between airfoils constructed around a deflected strut and target NACA-four digit airfoils has been obtained in terms of aerodynamic performance. It is clear that, by making use of nonlinear structural responses, camber control of deformable airfoils can be achieved by using a carefully designed preloaded internal spinal structure that moves through the desired shape changes under the control of a single actuator, delivering aerodynamic characteristics that match a set of prespecified target shapes. Studies that extend this approach to entire wings using buckling plates to form the central spine are currently underway. These schemes provide complete wing reshaping with just two force inputs, one to control camber and the other twist.

Acknowledgment

This research was supported by a grant from the Faculty of Engineering, Science and Mathematics at the University of Southampton.

References

[1] Khot, N. S., "Deformation of a Flexible Wing Using an Actuating System for a Rolling Maneuver Without Ailerons," AIAA Paper 98-1802, 1998.

[2] Gern, F. H., Inman, D. J., and Kapania, R. K., "Structural and Aeroelastic Modeling of General Planform Wings With Morphing Airfoils," *AIAA Journal*, Vol. 40, No. 4, April 2002, pp. 628–637.

[3] Anderson, J. D., *Introduction to Flight*, McGraw–Hill, New York, 1978.

[4] Austin, F., Rossi, M. J., Van Nostrand, W., Gareth, K., and Jameson, A., "Static Shape Control for Adaptive Wings," *AIAA Journal*, Vol. 32, No. 9, Sept. 1994, pp. 1985–1901.

[5] Chatlynne, E., Rumingny, N., Amitay, M., and Glezer, A., "Virtual Aero-Shaping of a Clark-Y Airfoil Using Synthetic Jet Actuators," AIAA Paper 2000-0732, 2000.

[6] Chen, F. J., and Beeler, G. B., "Virtual Shaping of a Two-Dimensional NACA 0015 Airfoil Using Synthetic Jet Actuator," AIAA Paper 2002-3273, 2002.

[7] Seifert, A., Eliahu, S., Greenblatt, D., and Wygnanski, I., "Use of Piezoelectric Actuators for Airfoil Separation Control," *AIAA Journal*, Vol. 36, No. 8, Aug. 1998, pp. 1535–1536.

[8] Munday, D., and Jacob, J., "Active Control of Separation on a Wing with Conformal Camber," AIAA Paper 2001-0293, Jan. 2001.

[9] Balas, M. J., "Optimal Quasi-Static Shape Control for Large Aerospace Antennae," *Journal of Optimization Theory and Applications*, Vol. 46, No. 2, 1985, pp. 153–170.

[10] Yoon, H. S., Washington, G., and Theunissen, W. H., "Analysis and Design of Doubly Curved Piezoelectric Strip-Actuated Aperature Antennas," *IEEE Transactions on Antennas and Propagation*, Vol. 48, No. 5, May 2000, pp. 755–763.

[11] Saggere, L., and Kota, S., "Static Shape Control of Smart Structures Using Compliant Mechanisms," *AIAA Journal*, Vol. 37, No. 5, May 1999, pp. 572–578.

[12] Lu, K. J., and Kota, S., "Synthesis of Shape Morphing Compliant Mechanisms Using a Load Path Representation Method," *Smart Structures and Materials 2003: Modeling, Signal Processing and Control, Proceedings of SPIE*, edited by R. C. Smith, Vol. 5049, International Society for Optical Engineering, Bellingham, WA, 2003, pp. 337–348.

[13] Natarajan, A., Kapania, R. K., and Inman, D. J., "Aeroelastic Optimization of Adaptive Bumps for Yaw Control," *Journal of Aircraft*, Vol. 41, No. 1, Jan.–Feb. 2004.

[14] Scott, W., "Performance Gains Confirmed in Mission Adaptive Wing Tests," *Aviation Week and Space Technology*, Vol. 129, No. 77, 1988, p. 77.

[15] Pendleton, E., Bessette, D., Field, P., Miller, G., and Griffin, K., "Active Aeroelastic Wing Flight Research Program: Technical Program and Model Analytical Development," *Journal of Aircraft*, Vol. 37, No. 4, July–Aug. 2000, pp. 554–561.

[16] Gano, S. E., Renaud, J. E., Batill, S. M., and Tovar, A., "Shape Optimization for Conforming Airfoils," AIAA Paper 2003-1579, April 2003.

[17] Abdulrahim, M., Garcis, H., and Lind, R., "Flight Characteristic of Shaping the Membrane Wing of a Micro Air Vehicle," *Journal of Aircraft*, Vol. 42, No. 1, Jan.–Feb. 2005, pp. 131–137.

[18] Ursache, N. M., Bressloff, N. W., and Keane, A. J., "The Design of Post-Buckled Spinal Structures for Airfoil Shape Control Using Optimization Methods," *Proceedings of 5th ASMO UK/ISSMO Conference on Engineering Design Optimization*, Leeds Univ. Press, Leeds, U.K., July 2004.

[19] Crisfield, M. A., *Non-linear Finite Element Analysis of Solids and Structures*, Vol. 1, John Wiley and Sons, Chichester, England, U.K., 1997.

[20] Wempner, G. A., "Discrete Approximations Related to Nonlinear Theory of Solids," *International Journal of Solids and Structures*, Vol. 7, No. 11, Nov. 1971, pp. 1581–1591.

[21] Riks, E., "The Application of Newton's Method to the Problem of Elastic Stability," *Journal of Applied Mechanics*, Vol. 39, 1972, pp. 1060–1065.

[22] Haftka, R. T., Prasad, B., "Optimum Structural Design with Plate Bending Elements—A Survey," *AIAA Journal*, Vol. 19, No. 4, 1981, pp. 517–522.

[23] Zhou, M., Gu, Y. X., and Rozvany, G. I. N., "Application of DCOC method to Plates and Shells," *Proceedings of the First World Congress of Structural and Multidisciplinary Optimization*, edited by N. Olhoff and G. N. Rozvany, Elsevier Science, Oxford, 1995, pp. 25–32.

[24] Olhoff, N., Krog, L. A., and Lund, E., "Optimization of Multimodal Eigenvalues," *Proceedings of the First World Congress of Structural and Multidisciplinary Optimization*, edited by N. Olhoff and G. N. Rozvany, Elsevier Science, Oxford, 1995, pp. 701–708.

[25] Bochenek, B., "On Postbuckling Constraints in Structural Optimization Against Instability," *Proceedings of the First World Congress of Structural and Multidisciplinary Optimization*, edited by N. Olhoff and G. N. Rozvany, Elsevier Science, Oxford, 1995, pp. 717–724.

[26] Bernitsas, M. M., and Suryatama, D., "Structural Redesign by Large Admissible Perturbations with Static Mode Compensation," *Journal of Offshore Mechanics and Arctic Engineering*, Vol. 121, No. 1, 1999, pp. 39–46.

[27] Blouin, V. Y., and Bernitsas, M. M., "Redesign of Submerged Structure by Large Admissible Perturbations," *Journal of Offshore Mechanics and Arctic Engineering*, Vol. 123, No. 3, 2001, pp. 102–111.

[28] Lighthill, M. J., "A New Method for Two-Dimensional Aerodynamic Design," Aeronautical Research Council Reports and Memoranda No. 1111, 1945.

[29] Daripa, P. K., "On Applications of a Complex Variable Method in Compressible Flows," *Journal of Computational Physics*, Vol. 88, No. 2, 1990, pp. 337–361.

[30] Stanitz, J. D., "General Design Method for Three-Dimensional, Potential Flow Fields," NASA Technical Report CR 3288, 1990.

[31] Zannetti, L., "A Natural Formulation for the Solution of Two-Dimensional or Axis-symmetric Inverse Problems," *International Journal of Numerical Methods in Engineering*, Vol. 22, No. 2, 1986, pp. 451–463.

[32] Chaviaropoulos, P., Dedoussis, V., and Papailiou, K. D., "Compressible Flow Airfoil Design Using Natural Coordinates," *Computer Methods in Applied Mechanics and Engineering*, Vol. 110, Nos. 1–2, Dec. 1993, pp. 131–142.

[33] Giles, M. B., and Drela, M., "Two-Dimensional Transonic Aerodynamic Design Method," *AIAA Journal*, Vol. 25, No. 9, 1987, pp. 1199–1206.

[34] Drela, M., and Giles, M. B., "Viscous-Inviscid Analysis of Transonic and Low Reynolds Number Airfoils," *AIAA Journal*, Vol. 25, No. 10, 1987, pp. 1347–1355.

[35] Campbell, R. L., "Efficient Viscous Design of Realistic Aircraft Configurations," AIAA Paper 98-2593, 1998.

[36] Milholen, W. E., "An Efficient Inverse Aerodynamic Design Method for Subsonic Flows," AIAA 2000-0780, 2000.

[37] Keane, A. J., and Nair, P. B., *Computational Methods for Aerospace Design: The Pursuit of Excellence*, John Wiley and Sons, Chichester, England, U.K., 2005.

[38] Samareh, J. A., "Survey of Shape Parameterization Techniques for High-Fidelity Multidisciplinary Shape Optimization," *AIAA Journal*, Vol. 39, No. 5, 2001, pp. 877–883.

[39] Schram, U., and Pilkey, W. D., "The Application of Rational B-Splines for Shape Optimization," *Proceedings of the First World Congress of Structural and Multidisciplinary Optimization*, edited by N. Olhoff and G. N. Rozvany, Elsevier Science, Oxford, 1995, pp. 377–382.

[40] Farin, G., *Curves and Surfaces for Computer-Aided Geometric Design: A Practical Guide*, Academic Press, London, 1992.

[41] VGK Method for Two-Dimensional Aerofoil Sections, Ver. 2.0, ESDU 96028, ESDU 96029, ESDU International, London, 1997.

[42] Cai, J., and Liu, F., "Static Aero-elastic Computation with a Coupled CFD and CSD Method," AIAA Paper 01-0717, 2001.

[43] Alonso, J. J., LeGresley, P., van der Weide, E., "High-Fidelity Multi-Disciplinary Optimization," AIAA Paper 2004-4480, 2004.

[44] Keane, A. J., "Wing Optimization Using Design of Experiment, Response Surface, and Data Fusion Methods," *Journal of Aircraft*, Vol. 40, No. 4, 2003, pp. 741–750.

M. Ahmadian
Associate Editor